Inhomogeneous Relaxation of a Molecular Layer on an Insulator due to Compressive Stress

F. Bocquet,[1] L. Nony,[1,*] S. C. B. Mannsfeld,[2] V. Oison,[1] R. Pawlak,[1] L. Porte,[1] and Ch. Loppacher[1]

[1]*Aix-Marseille Université, IM2NP, Avenue Normandie-Niemen Case 151, F-13397 Marseille CEDEX 20, France; CNRS, IM2NP (UMR 7334), Marseille-Toulon, France*

[2]*Stanford Synchrotron Radiation Laboratory (SSRL), Stanford, CA 94305, USA*

(Received 5 January 2012; published 16 May 2012)

We discuss the inhomogeneous stress relaxation of a monolayer of hexahydroxytriphenylene (HHTP) which adopts the rare line-on-line (LOL) coincidence on KCl(001) and forms moiré patterns. The fact that the hexagonal HHTP layer is uniaxially compressed along the LOL makes this system an ideal candidate to discuss the influence of inhomogeneous stress relaxation. Our work is a combination of noncontact atomic force microscopy experiments, density functional theory and potential energy calculations, and a thorough interpretation by means of the Frenkel-Kontorova model. We show that the assumption of a homogeneous molecular layer is not valid for this organic-inorganic heteroepitaxial system since the best calculated energy configuration correlates with the experimental data only if inhomogeneous relaxations of the layer are taken into account.

DOI: 10.1103/PhysRevLett.108.206103 PACS numbers: 68.37.Ps, 33.15.Fm, 68.43.Hn, 68.60.Bs

Highly ordered π-conjugated organic thin films grown on surfaces by molecular beam epitaxy represent a rewarding approach to new classes of heterojunctions for organic semiconductors with promising applications in optoelectronics [1]. In this regard, physisorption of organic molecules on *insulating substrates* is of inherent interest. Little is known about organic-inorganic heteroepitaxy (OIHE) on single-crystal insulators since only a few systems have been investigated thus far, and most of them on alkali halide substrates [2–5]. OIHE is governed by a delicate balance between molecule-molecule interactions involving supramolecular interactions, and molecule-substrate interactions. For polar molecules on alkali halides the latter are a combination of van der Waals (vdW) interactions acting like an unstructured background, and electrostatic (ES) interactions governed by the periodicity of the ionic surface. If the physisorption of large molecular layers on insulators is mainly driven by vdW interactions, then the layer can be regarded as a floating, i.e., with no particular anchoring sites, 2D periodic overlayer with a structure close to a crystallographic plane of the organic bulk crystal. However, if the ES interaction becomes significant, site-specific adsorption can determine the growth mode [2,3]. In this case, the organic overlayer adsorbs on the substrate in the best lattice match. This process does not necessarily generate a commensurate molecular supercell, but may promote more complex epitaxies such as the line-on-line (LOL) epitaxy [6–8]. Although coincidence between the organic layer and the substrate maximizes its adsorption energy (stabilizing effect), it may also introduce stress within the layer (destabilizing effect). For systems with large misfit between adsorbate bulk and substrate lattices, the stress may become so large that the layer becomes unstable and dewetting takes place [3]. For intermediate misfits, efficient stress release may be achieved by local relaxations within the layer (nearest neighbor scale) which would provoke the layer to deviate from its periodic, and hence homogeneous, 2D bulk structure. This is known to occur in metallic heterostructures by means of misfit dislocations. Surprisingly, for OIHE where conformational adaptation and relative flexibility of the supramolecular network might favor local inhomogeneity, to our knowledge few attempts have been made to account for this effect [9,10].

In this Letter, we study the model system 2, 3, 6, 7, 10, 11 hexahydroxytriphenylene (HHTP)/KCl(001) in which the molecular monolayer is not dewetting despite an uniaxial compression of 4%. We demonstrate that such a large compressive stress can be energetically favorable if local, inhomogeneous relaxations are taken into account. These are treated within the framework of the 1D Frenkel-Kontorova (FK) model [11].

HHTP [see inset in Fig. 1(a)] is a planar molecule with threefold symmetry and six peripheral hydroxyl groups. Crystallographic data are only reported for the hydrated crystal which forms a monoclinic unit cell (u.c.) [12]. HHTP is known as a prototypical discotic liquid crystal [13]. Its discotic nature combined with its hydroxyl groups make it well-suited to promote 2D self-organization. Indeed, on metals HHTP forms extended and highly organized layers which are linked by supramolecular [14], or covalent interactions [15].

Submonolayers of HHTP were evaporated on KCl(001) single crystals in ultrahigh vacuum according to standard procedure (see, e.g., Ref. [5] and Supplemental Material [16] for details) and imaged at room temperature by noncontact atomic force microscopy (nc-AFM). HHTP forms stable and extended 2D molecular monolayers which exhibit three orientations [see arrows 1, 2, and 3 in Fig. 1(a)]. The apparent height of the layers is 370 pm,

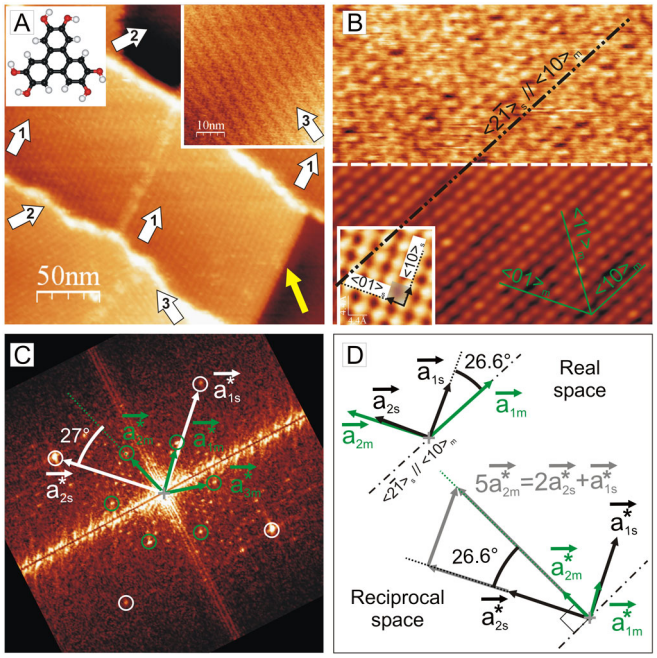

FIG. 1 (color online). (a) Molecular domains of HHTP on KCl (001) (300×300 nm^2, normalized Δf: $\gamma = -0.03$ nN $\cdot \sqrt{\text{nm}}$). The domains consist of fringes forming a moiré pattern with a periodicity of 45.5 Å. Three distinct orientations are visible (numbered arrows). Insets: HHTP molecule (left) and zoom on a type 3 domain showing both the fringes orientation and a molecular axis (right, 40×40 nm^2, $\gamma = -0.12$ nN $\cdot \sqrt{\text{nm}}$). (b) Zoom on a molecular domain (25×25 nm^2, $\gamma = -0.27$ nN $\cdot \sqrt{\text{nm}}$). Upper part: acquired topography signal. Lower part: topography signal autocorrelation showing the molecular hexagonal arrangement in a LOL epitaxy ($\langle 10\rangle_m$ and $\langle 2\bar{1}\rangle_s$ are parallel). Inset: KCl imaged close to the molecular domain (2.2×2.2 nm^2, $\gamma = -0.33$ nN $\cdot \sqrt{\text{nm}}$). (c) FFT showing both the diffraction spots of HHTP and of KCl (green and white circles, respectively): raw data in Fig. S1 of Supplemental Material [16]. (d) Sketch illustrating the correspondence between real and reciprocal space. The LOL results from a coincidence of the ends of molecular and substrate reciprocal vectors: $5\mathbf{a}^*_{\mathbf{2m}} = 2\mathbf{a}^*_{\mathbf{2s}} + \mathbf{a}^*_{\mathbf{1s}}$.

which indicates that molecules are lying flat on the substrate. Henceforth, all crystallographic axes related to the substrate and the molecular overlayer are subscripted s and m, respectively; the KCl(001) surface is described by its square primitive u.c. High-resolution images, i.e., properly drift corrected and rescaled with respect to the KCl (001) u.c., acquired on different domains reveal the same quasihexagonal molecular arrangement [see Fig. 1(b)]. Soft image processing (FFT and autocorrelation) permits to accurately measure the molecular u.c.: $\mathbf{a_{1m}}$ (along $\langle 10\rangle_m$) measures $\|\mathbf{a_{1m}}\| = (11.0 \pm 0.3)$ Å, and $\mathbf{a_{2m}}$ (along $\langle 01\rangle_m$) measures $\|\mathbf{a_{2m}}\| = (11.5 \pm 0.3)$ Å. The angle between these vectors is $(\widehat{\mathbf{a_{1m}}, \mathbf{a_{2m}}}) = (120 \pm 3)°$. Combined analysis in the reciprocal and direct space [see Figs. 1(b)–1(d)] shows that the $\mathbf{a_{1m}}$ vector is $-(27 \pm 3)°$ tilted with respect to the $\langle 10\rangle_s$ axis. This direction matches the $\langle 2\bar{1}\rangle_s$ axis, the exact orientation of which is given by $-26.6°$. Therefore, the dense $\langle 10\rangle_m$ molecular rows exactly lie on non primitive $\langle 2\bar{1}\rangle_s$ substrate rows. Moreover, the distance between two adjacent $\langle 10\rangle_m$ rows, $d_m = \|\mathbf{a_{2m}}\| \cos(30°) = 9.96$ Å, matches within 0.1% the distance between five substrate $\langle 2\bar{1}\rangle_s$ rows [see Fig. 1(d), the distance between adjacent $\langle 2\bar{1}\rangle_s$ rows is $d_s = 4.45/\sqrt{2^2 + 1^2} = 1.99$ Å, where 4.45 Å is the u.c. parameter of KCl(001), hence $5 \times d_s = 9.95$ Å]. The epitaxy of HHTP on KCl(001) is therefore an exact LOL epitaxy [7,8] with $\langle 10\rangle_m \| \langle 2\bar{1}\rangle_s$.

Striking features of the experimental images are the periodic fringes that appear in the domains and form well-defined moiré patterns with a periodicity of $a_M = (45.5 \pm 1)$ Å and a tilt of $(100 \pm 3)°$ with respect to the $\langle 10\rangle_m$ axis [see Figs. 1(a) and 2(a)]. These domains are all equivalent as their relative orientations can be deduced by applying the symmetry element of the punctual group of the substrate. A recurrent observation is that domain borders (strong adsorption sites) are not oriented along dense molecular rows, but rather along moiré fringes [see yellow arrow in Fig. 1(a)], which suggests that the fringes result from coincidences (or quasicoincidences) between the molecular and the substrate lattice points. To address that issue, simulations of the moiré pattern were performed by superposing the HHTP and KCl lattices [7] [see Fig. 2(b)]. The contrast of the resulting pattern spreads from black (100% coincident) to white (0% coincident). To properly reproduce the experimental moiré pattern (periodicity and orientation of the fringes), the molecular u.c. has to be set to $\|\mathbf{a}^{\text{sim}}_{\mathbf{1m}}\| = 11.15$ Å, $\|\mathbf{a}^{\text{sim}}_{\mathbf{2m}}\| = 11.28$ Å, and $(\widehat{\mathbf{a}^{\text{sim}}_{\mathbf{1m}}, \mathbf{a}^{\text{sim}}_{\mathbf{2m}}}) = 118.1°$. This structure depicts a slightly distorted hexagonal arrangement, in agreement with the experimental data and the LOL epitaxy. Any tiny change of these values drastically changes the simulated pattern which then becomes incompatible with the experimental fringes. Both the moiré fringes and the bright spots visible in the autocorrelation images [circles in Fig. 2(a)] are reproduced in the simulated pattern, which therefore testifies that quasicoincidences occur between the molecular overlayer and the substrate lattice points.

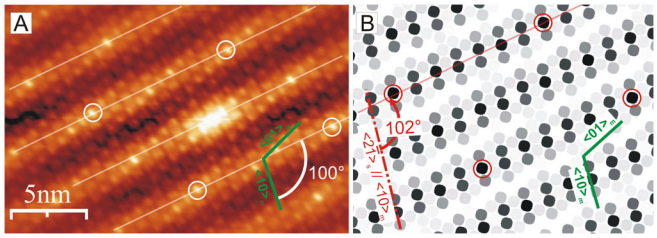

FIG. 2 (color online). (a) Autocorrelation image of a molecular domain showing moiré fringes and periodic bright spots. The orientation of the fringes with respect to $\langle 10\rangle_m$ is $(100 \pm 3)°$. (b) Simulated moiré pattern which reproduces both the experimental fringes and the bright spots, respectively.

To investigate the energy configuration of the layer, density functional theory (DFT) and potential energy (PE) calculations were carried out [see Figs. 3 and Supplemental Material [16]]. DFT calculations give the most stable molecular conformation and its corresponding freestanding layer configuration [see inset in Figs. 1(a) and 3(a), respectively]. The molecules assemble in a planar and regular hexagonal u.c. via three H bonds. No molecular orbitals hybridization takes place but partial charges are present within the molecule (see Supplemental Material [16]). The cohesion energy of the structure is $E_{\mathrm{coh},0} = -0.36$ eV/molecule and its uniaxial stiffness along the $\langle 10\rangle_m$ axis is estimated to be $k_{\mathrm{DFT}} = 15.3$ N/m [fit of the data shown in Fig. 3(b) with a harmonic potential]. The parameters of the u.c. optimized by DFT are $\|\mathbf{a}^{\mathrm{DFT}}_{\mathbf{1m},\mathbf{2m}}\| = 11.62$ Å and $(\widehat{\mathbf{a}^{\mathrm{DFT}}_{\mathbf{1m}}, \mathbf{a}^{\mathrm{DFT}}_{\mathbf{2m}}}) = 120°$. *A posteriori*, the experimentally observed LOL epitaxy can now be justified since the distance between two dense molecular rows of the freestanding layer, $\|\mathbf{a}^{\mathrm{DFT}}_{\mathbf{2m}}\| \cos(30°) = 10.06$ Å, fits within 1% to five distances between two adjacent $\langle 2\bar{1}\rangle_s$ rows. However, unlike other molecular films on KCl [5], the equilibrium configuration of the freestanding layer does not match the experimental one along the $\langle 2\bar{1}\rangle_s$ direction, but shows a significant discrepancy with a compressive stress of $(a^{\mathrm{sim}}_{1m} - a^{\mathrm{DFT}}_{1m})/a^{\mathrm{DFT}}_{1m} = -4.0\%$.

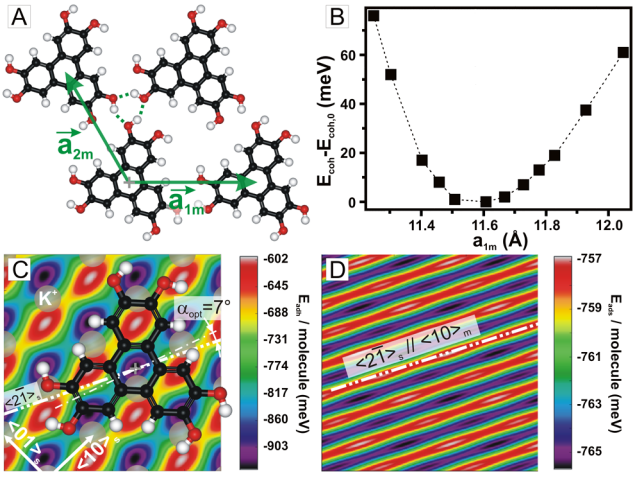

FIG. 3 (color online). (a) Unit cell of the HHTP freestanding layer as calculated by DFT. A H-bonded (dotted green lines) hexagonal structure with $\|\mathbf{a}^{\mathrm{DFT}}_{\mathbf{1m},\mathbf{2m}}\| = 11.62$ Å is found. (b) Evolution of the cohesion energy per molecule as a function of a^{DFT}_{1m} (uniaxial stress), from which the uniaxial stiffness $k_{\mathrm{DFT}} = 15.3$ N/m of the layer is derived. (c) Adhesion energy of a single HHTP adsorbed on KCl(001), as calculated by PE calculations. The constant background of -0.76 eV (mainly vdW interaction) is laterally corrugated due to ES molecule-substrate interaction. (d) Adsorption energy per molecule for a cluster of 3600 molecules when translated with fixed angular orientation. The remaining 1D potential is 4 meV deep and carries the LOL epitaxy direction.

Such a 4% uniaxial compressive stress is unexpected since (i) along the LOL direction, an almost perfect geometric coincidence could be achieved for seven molecules (6×11.62 Å) lying over eight substrate ions along the $\langle 2\bar{1}\rangle_s$ axis (7×9.95 Å) giving a nearly unstressed layer (0.1% misfit), and (ii) the stress-induced elastic energy stored in the layer decreases by a large amount (35%) the cohesive energy with respect to the freestanding overlayer $[E_{\mathrm{el}} = \frac{1}{2} k_{\mathrm{DFT}}(a^{\mathrm{sim}}_{1m} - a^{\mathrm{DFT}}_{1m})^2 = 0.112$ eV]. Only a sufficiently large and in-plane corrugated molecule-substrate ES interaction could explain the observed compression.

As both large clusters and interactions with an ionic substrate are properly treated by PE calculations [7,17], we proceeded as follows. First, the freestanding layer was calculated. The PE results are in excellent agreement with the DFT calculations. Second, the adhesion energy for a single molecule kept at its optimal orientation, $\alpha_{\mathrm{opt}} = 7°$ with respect to $\langle 2\bar{1}\rangle_s$, is calculated for different lateral positions [see Fig. 3(c)]. The obtained energy landscape can be interpreted as a constant vdW background of -0.76 eV plus a locally modulated part of ± 0.24 eV due to ES interactions. Third, calculations involving a large cluster (3600 molecules) were done using the values derived from the simulated moiré pattern as input parameters. This structure corresponds to a local energetic minimum and gives the energy landscape shown in Fig. 3(d) when all 3600 molecules are translated in block over the surface. The low energetic corrugation (4 meV) perpendicularly to the $\langle 2\bar{1}\rangle_s$ axis is sufficiently large to promote the LOL epitaxy [7]. However, when this structure is fully relaxed in order to find an absolute minimum, the calculations converge towards the quasi freestanding layer with the LOL orientation maintained. Therefore the PE method, which strictly describes a homogeneous cluster, fails to predict the experimental stress along the $\langle 10\rangle_m$ axis. One possibility to relieve such stress is to consider a pseudo-periodic, inhomogeneous, 2D molecular structure. Describing large molecular domains with 2D local relaxations, including eventually variable orientations (α), is out of the scope of this letter. Nevertheless, as the experimentally observed stress is uniaxial, we can at least semiquantitatively discuss the problem in the 1D FK formalism [11], the details of which are given in Supplemental Material [16].

The purpose of the FK model is to find the best equilibrium configuration for a set of harmonically interacting "point masses" (here molecules initially separated by 11.62 Å) constrained in a 1D periodic potential (here the ES potential) by taking into account local variations of next neighbor distances. We assume the overlayer as a set of $\langle 10\rangle_m$ noninteracting parallel and uniaxially compressed 1D molecular chains. Along one chain, two next neighbors are linked by a spring with stiffness $k = k_{\mathrm{DFT}}/3$ because a molecule possesses only two neighbors, despite six in the u.c. The molecules are exposed to an ES potential given by the one taken along the $\langle 2\bar{1}\rangle_s$ axis in Fig. 3(c) and shown in

Fig. 4. Its periodicity a is obviously 9.95 Å. In order to simplify the approach, the potential is fitted by a sinusoidal curve with a peak-to-peak amplitude $W = 0.40$ eV (see Supplemental Material [16]). The key parameter of the FK model which compares the elastic and the adsorption energy is given by $l_0^{\text{theo}} = \sqrt{ka^2/2W} = 6.4$. Along the $\langle 2\bar{1}\rangle_s$ direction, each molecule in the chain is supposed to be identically oriented, i.e., with the optimal angle α_{opt}. Note that any local orientational variation (within a range of, e.g., $\pm 5°$) between two adjacent molecules may additionally increase the adsorption energy [18], which should be considered for further studies.

According to the data needed to simulate the moiré pattern (i.e., with an intermolecular distance of 11.15 Å), we force 4% compression along a molecular chain by distributing nine molecules on ten ES potential minima along the $\langle 2\bar{1}\rangle_s$ axis (8×11.62 Å on 9×9.95 Å). This yields $l_0 = 4.0$ and an averaged intermolecular distance of 11.19 Å instead of $l_0^{\text{theo}} = 6.4$ and 11.15 Å, respectively. The FK model gives the calculated positions of the molecules along the potential as depicted in Fig. 4. Note that the local relaxation is reflected by a regular alternation of always two shortened and two prolonged intermolecular distances along the stressed line . The energy per molecule of this relaxed configuration is $E_{\text{rel}}^{(1)} = -34$ meV, while for an homogeneously 4% compressed chain, it is $E_{\text{hom}} = 10$ meV. Therefore the inhomogeneous relaxation allows for an energy gain of $(E_{\text{hom}} - E_{\text{rel}}^{(1)}) \simeq 44$ meV per molecule. The ultimate test to validate our model of inhomogeneous relaxation is to see whether the structure displayed in Fig. 4 remains energetically favorable compared to a nearly unstressed one (seven molecules over eight substrate periods along the $\langle 2\bar{1}\rangle_s$ axis). For this structure, the FK model yields $l_0 = 8.7$ and inhomogeneous relaxation with an energy gain $E_{\text{rel}}^{(2)} = -6$ meV. Therefore, the energetically most favorable molecular structure is the 4% compressed, inhomogeneously relaxed layer, which is compliant with the experimental data.

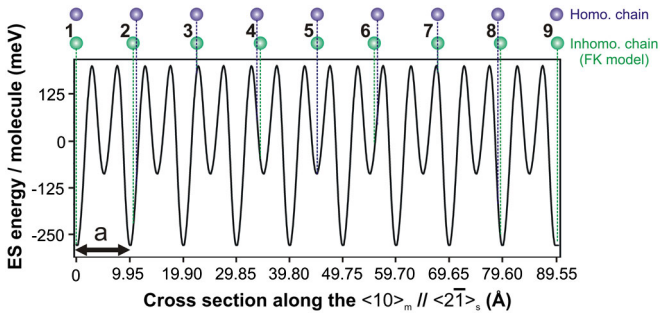

FIG. 4 (color online). Nine molecules are forced within the distance of ten minima of the ES energy profile along the $\langle 2\bar{1}\rangle_s$ for a single molecule [see Fig. 3(c)]. The adsorption energy of the molecules with even number is significantly larger when the molecules are spaced according to the FK model (lower ones) compared to the equally spaced molecules (upper ones, homogeneous chain).

In conclusion, we studied the adsorption of a monolayer of HHTP on KCl(001). To our knowledge, this is the first example where an organic layer adopts the rare LOL epitaxy on an ionic substrate. The fact that the hexagonal HHTP layer is uniaxially compressed along the LOL direction made this system an ideal candidate to discuss the influence of stress-induced local relaxation, a point which has been neglected in organic overlayers. Our results demonstrate that the observed compression of the organic layer becomes energetically favorable only if local inhomogeneous relaxations are considered. More generally, the adsorption energy of a large molecular cluster in a LOL epitaxy does not vary upon changes of the molecular positions along the LOL [see Fig. 3(d)]. Thus, local relaxations are facilitated along this direction. The main criterion for the formation of a LOL epitaxy is that along the other molecular directions, the distance between dense molecular rows of the freestanding layer and the one between substrate rows match closely.

F. B., L. N., and C. L. thank S. Clair and J.-M. Themlin for useful discussions and acknowledge support from the ANR and the PNano MolSiC (ANR-08-P058-36) and Nanokan (ANR-11-BS10-004) programs. This work was done in part at Stanford Synchrotron Radiation Lightsource (SSRL), operated by Department of Energy.

*Corresponding author.
laurent.nony@im2np.fr.

[1] R. Otero, J. M. Gallego, A. L. Vázquez de Parga, N. Martín, and R. Miranda, Adv. Mater. **23**, 5148 (2011).
[2] T. Dienel, C. Loppacher, S. C. B. Mannsfeld, R. Forker, and T. Fritz, Adv. Mater. **20**, 959 (2008).
[3] S. Burke, W. Ji, J. M. Mativetsky, J. M. Topple, S. Fostner, H.-J. Gao, H. Guo, and P. Grütter, Phys. Rev. Lett. **100**, 186104 (2008).
[4] D.-M. Smilgies and E. J. Kintzel, Phys. Rev. B **79**, 235413 (2009).
[5] R. Pawlak, L. Nony, F. Bocquet, V. Oison, M. Sassi, J.-M. Debierre, C. Loppacher, and L. Porte, J. Phys. Chem. C **114**, 9290 (2010).
[6] D. Hooks, T. Fritz, and M. Ward, Adv. Mater. **13**, 227 (2001).
[7] S. Mannsfeld, K. Leo, and T. Fritz, Phys. Rev. Lett. **94**, 056104 (2005).
[8] D. Kasemann, C. Wagner, R. Forker, T. Dienel, K. Mullen, and T. Fritz, Langmuir **25**, 12 569 (2009).
[9] V. Oison, M. Koudia, M. Abel, and L. Porte, Phys. Rev. B **75**, 035428 (2007).
[10] P. Fenter, P. Eisenberger, P. Burrows, S. R. Forrest, and K. S. Liang, Physica (Amsterdam) **221B**, 145 (1996).
[11] Y. I. Frenkel and T. Kontorova, Zh. Eksp. Teor. Fiz. **8**, 1340 (1938).
[12] T. Andresen, F. Krebs, N. Thorup, and K. Bechgaard, Chem. Mater. **12**, 2428 (2000).

[13] D. Adam, F. Closs, T. Frey, D. Funhoff, D. Haarer, P. Schuhmacher, and K. Siemensmeyer, Phys. Rev. Lett. **70**, 457 (1993).

[14] R. Pawlak, S. Clair, V. Oison, M. Abel, O. Ourdjini, N. A. A. Zwaneveld, D. Gigmes, D. Bertin, L. Nony, and L. Porte, Chem. Phys. Chem. **10**, 1032 (2009).

[15] N. Zwaneveld, R. Pawlak, M. Abel, D. Catalin, D. Gigmes, D. Bertin, and L. Porte, J. Am. Chem. Soc. **130**, 6678 (2008).

[16] See Supplemental Material at http://link.aps.org/supplemental/10.1103/PhysRevLett.108.206103 for details about the experimental, computational, and FK methods.

[17] S. Mannsfeld and T. Fritz, Phys. Rev. B **71**, 235405 (2005).

[18] J.-Z. Wang, M. Lan, T.-N. Shao, G.-Q. Li, Y. Zhang, C.-Z. Huang, Z.-H. Xiong, X.-C. Ma, J.-F. Jia, and Q.-K. Xue, Phys. Rev. B **83**, 235433 (2011).